Available online at www.sciencedirect.com

ScienceDirect

Energy Procedia 137 (2017) 477–486

Energy Procedia

www.elsevier.com/locate/procedia

14th Deep Sea Offshore Wind R&D Conference, EERA DeepWind'2017, 18-20 January 2017, Trondheim, Norway

A full-scale 3D Vs 2.5D Vs 2D analysis of flow pattern and forces for an industrial-scale 5MW NREL reference wind-turbine.

Mandar Tabib[a,*], Adil Rasheed[a], M. Salman Siddiqui[b], Trond Kvamsdal[b]

[a]*Mathematics and Cybernetics, SINTEF Digital, Strindveien 4, 7035, Trondheim, Norway.*
[b]*Department of Mathematical Sciences,Faculty of Information Technology and Electrical Engineering,NTNU,Trondheim,Norway.*

Abstract

NREL 5MW reference turbine, which is a popular, realistic and standardized industrial scale offshore turbine model, is used in this work for understanding the associated flow-complexities and for testing models. For such full-scale wind-turbine, the wish list is towards a accurate real-time prediction for better control and monitoring. Here, models like 2D based strip-theory [1] can help, but the extent of its applicability can be understood through a comparative performance of 2D Vs 2.5D Vs 3D CFD models. A stand-still blade condition is chosen for this study which can arise in a wind-farm when both yaw and pitch regulations are off-line. Further, even this simple stand-still condition is expected to have complex 3D effects due to blade geometry and due to the non-optimized conditions (blades twist being optimized for rotation). For such cases, the current work compares flow-profiles and forces computed by a 3D, 2.5D and 2D CFD models along the different sections of the NREL 5 MW turbine. The 2D CFD results are compared with experimentally measured drag and lift coefficient values as reported in DOWEC report [2]. The results from this study indicates that the flow close to the hub is dominated by complex 3D structures and unsteadiness while the three dimensionality and unsteadiness diminish as one moves away from the hub and towards the tip so much so that 2D simulations are sufficient for a faithful representation of the flow behavior. However, closer to the hub 2D simulations can not be utilized without adequate corrections. The work has implications for the 2D based approaches like strip-theory.

Peer-review under responsibility of SINTEF Energi AS.

Keywords: CFD; wind turbine; 5MW NREL; 3D; 2.5D; 2D.

1. Introduction and work objectives

1.1. Introduction

Wind-turbine blades comprising of multiple sections of different airfoil exhibit complex flow-patterns [3,4] along the blade length and generate wakes influencing wind-farm operation [5,6]. It is important to model the flow accurately for enabling efficient designs for not only turbines but also wind-farm layouts. However, conducting highly

* Corresponding author. Tel.: +4792011677.
E-mail address: mandar.tabib@sintef.no;adil.rasheed@sintef.no

1876-6102
Peer-review under responsibility of SINTEF Energi AS.
10.1016/j.egypro.2017.10.372

accurate flow simulations for industrial-scale turbine is time-consuming and industry often craves for faster-simulation methodologies. To meet up the expectations, computationally efficient approaches like 2D simulations based strip-theory [7] and blade element momentum method [8,9] has become the work horse in most of the relevant aerodynamic analysis lately. The approaches are based on analyzing only a few sections of the blade using two-dimensional computations and then interpolating / extrapolating between the sections to predict the aerodynamic characteristic of the full blade instead of doing a full fledged three dimensional computation. This banks on the assumption that the flow characteristics at different cross-sections are inherently two dimensional in nature, which might not necessarily be true at high Reynolds number flow and needs a thorough investigation. To this end the current work investigates the flow characteristics along a full scale stationary blade of a NREL 5MW reference turbine [10] using a 3D simulation. Additional 2D and 2.5D simulations are conducted for four different sections of the blade and compared against the 3D simulation results to evaluate the predictive capabilities of the simplified approach.

The NREL 5MW reference turbine [10] is chosen for this work, as it is a realistic and standardized industrial-scale off-shore turbine model. It is popularly used for testing new wind-turbine technologies, methodologies and numerical solvers by leading groups (several of U.S. DOEs Wind and Hydro-power Technologies Programs, EU's UpWind research program, and the International Energy Agency (IEA)'s Wind Annex XXIII Subtask Offshore Code Comparison Collaboration). The wind-turbine blade comprises of 8 sections (having shapes like Cylinder, DU21, DU25, DU30, DU35, DU40 and NACA 64 airfoils). The multiple-sections with diverse angles of attack provide an ideal opportunity to test and benchmark models and methodologies that can later be applied to solve a bigger range of industrial challenges. These multiple-segments impart a complex 3D geometry to the whole blade as the turbine-blade has span-wise variations of the chord length/blade thickness ratio as well as span-wise variations of blade twist. Hence, there is a need to understand the influence of these 3D effects in both stationary stand-still conditions as well as rotating conditions.

The current work focuses on simple stand-still aerodynamics, which may arise when both yaw and pitch regulations are off-line, say during the turbine-erection phase before the wind turbines are connected to the electrical grid. In the absence of a wind turbine control situation during off-line, the angles of attack of the flow on the blades are determined by the free wind direction, and the wind-turbine may operate outside the narrow normal operational range. Generally, wind-turbine blades are designed for rotating conditions, like , for example , a realistic turbine blade thickness is designed to taper from root to tip so as to enable the blade to withstand the higher stress and moment near the root than at the tip. Similarly, the blade twist is varied span-wise to maintain an optimum power coefficient (Cp) and similar angle of attack throughout blade-span. This geometric optimization works well in the rotating operational environment for which it is meant. However, in non-rotating environment (i.e. the stand-still aerodynamics condition), the blade twist optimized for rotation will make the flow artificially 3D compared to the actual rotor flow itself. Thus, in simple stand-still situations, complex 3D effects may exist owing to both the operating circumstances and the 3D complex turbine geometry. In these circumstances, it is important to understand in which regions the 2D simulations may be good enough. Hence, the main objectives of current work are listed as :

1.2. Objectives

1. Understanding variations in flow-complexity around different sections of the blade and the associated forces along the blade length from the hub to the tip.
2. Validation of simulated force coefficients results with reported measured results.
3. Developing recommendation regarding the applicability of 3D, 2.5D and 2D Computational Fluid Dynamics (CFD) analysis along different sections of the blade.

2. Approach and Methods

Three different CFD approaches (Full-scale 3D model vs 2.5D vs 2D model) are used in capturing the physics. To get a deeper intuition of flow behavior between the planar two dimensional and the full-scale three dimensional simulations, a 2.5D dimension is introduced. Initially, a full-scale 3D model (Figure 1) conducts simulation on the whole turbine-blade and then results are analyzed at different-sections as shown in Figure 1(b). The 2.5D segments are modeled from the full-scale 3D geometry by clipping the specific section from the full scale 3D model to include the

tapering effects along the radial direction. The 2.5D segment involves slip boundary condition at the walls parallel to the main stream-wise flow direction. Modeling this intermediate behavior enhances the intuition of the characteristic change in flow behavior from simple two dimension to complete three dimension. Furthermore, it also highlights the changes caused in the flow field by the bluntness of particular airfoil sections. The 2D simulation as the name suggests are conducted on specific 2D sections of the blade. All these computations are performed with consistent near-wall mesh conditions and computational domain size(figure 1) as described in the section 3.2. The chord-length and angle of attack for the four different airfoil blade segments are described in figure 3. Figure 2 shows different mesh tested for grid independence (as described in section 3.2). The final mesh used in simulation along with the location of four planes is in Figure 1(b). The 2D results are validated with reported measured drag and lift coefficient results in DOWEC report [2].

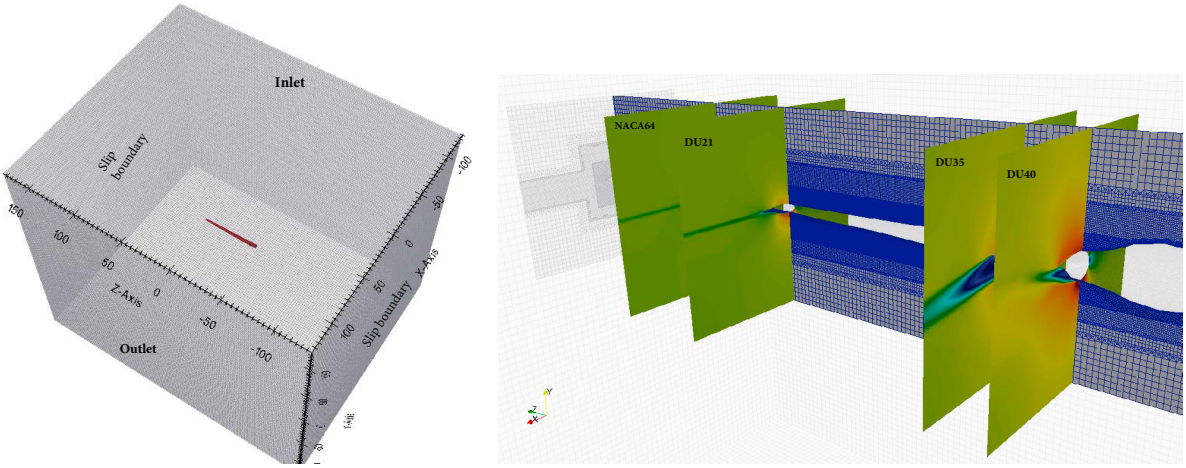

(a) Computational domain (b) Mesh and segments along the blade

Fig. 1. Computational domain and zoomed-in blade section

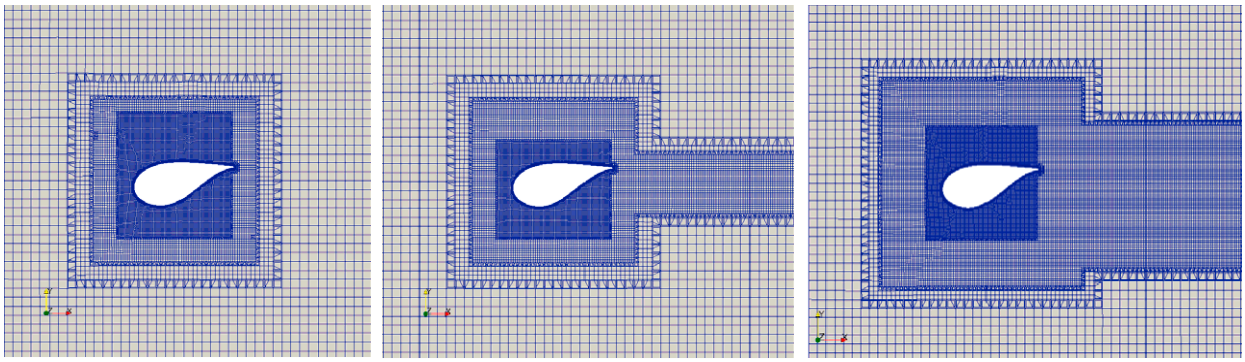

Fig. 2. Different mesh sizes considered for simulation of NREL 5MW reference turbine

Regarding the numerical model, all the three approaches use $k-\omega$ SST turbulence model[11,12] based on Reynolds Averaged Navier-Stokes. This model can help in better understanding of the flow behavior at different sections of the blade along its length starting from the hub and moving towards the tip. The model computes flow field and turbulence. The equation set comprises of time averaged mass continuity (Equation 1), momentum transport (Equation 2) and turbulence transport equations. The equations are described below in brief :

$$\nabla \cdot (\rho \mathbf{u}) = 0 \tag{1}$$

Segment	location of segment from hub, *m*	Angle of attack, ^{0}	Chord length, m
NACA-64	at z=44.55 m	α=3.12°	c=3.01 m
DU-21	at z=36.35 m	α=-5.36°	c= 3.50 m
DU-35	at z=15.85 m	α=-11.48°	c=4.65 m
DU-40	at z=11.75 m	α=-13.30°	c=4.55 m

Fig. 3. Details of each section that is studied in this work.

where ρ is the density.

$$\frac{D\mathbf{u}}{Dt} = -\nabla\left(\frac{p}{\rho}\right) + \frac{1}{\rho}\nabla\cdot\mathbf{R} + \mathbf{f} \tag{2}$$

where, operator $\frac{D}{Dt}$ refers to total derivative, operator ∇ refers to computing gradient, operator $\nabla\cdot$ refers to computing divergence, p is pressure, t is time, $\mathbf{R}$ is referred to turbulent stresses and arises owing to averaging procedure. Components of $\mathbf{R}$ can be computed as $R_{ij} = \nu_T\left(\frac{\partial u_i}{\partial x_j} + \frac{\partial u_j}{\partial x_i}\right) - \frac{2}{3}k\delta_{ij}$, where subscripts i, j refers to components of vector, k is turbulent kinetic energy and ν_T is turbulent diffusivity. The computation of eddy viscosity needed for the closure of above equation set is dependent upon the turbulence model (as described below). When $k-\omega$ model is used, the turbulent eddy viscosity is formulated in terms of turbulent kinetic energy (k) and specific dissipation (ω). The turbulent kinetic energy is obtained by solving equation 4 and specific dissipation is obtained by solving equation 5.

$$\mu_t = \frac{a_1 k}{max(a_1\omega, SF_1)} \tag{3}$$

$$\frac{Dk}{Dt} = \nabla\cdot\left(\frac{\nu_T}{\sigma_k}\nabla k\right) + P_k - \beta k\omega \tag{4}$$

$$\frac{D\omega}{Dt} = \nabla\cdot\left(\frac{\nu_T}{\sigma_e}\nabla\omega\right) + P_k\frac{\gamma}{\nu_T} - \beta\omega^2 + 2(1-F_1)\nabla\omega\nabla k\frac{\sigma_{w2}}{\omega} \tag{5}$$

where σ_e and σ_e are turbulent prandtl numbers, P_k is production of turbulent kinetic energy due to shear.

$$P_k = \nu_T\left(\frac{\partial u_i}{\partial x_j} + \frac{\partial u_j}{\partial x_i}\right)\frac{\partial u_i}{\partial x_j} \tag{6}$$

3. Simulation methodology : Solver details and set-up parameters

3.1. Solver details

The solver is created in OpenFOAM-2.3.0 (OF). To ensure continuity, OF uses an elliptic equation for the modified pressure which involves combining the continuity equation with divergence of momentum equation. This elliptic equation along with the momentum equation, energy equation and turbulence equation are solved in a segregated manner using the PISO-SIMPLE algorithm (PIMPLE algorithm). The PIMPLE algorithm allows use of a bigger time step for transient simulations. The OF uses a finite volume discretization technique, wherein all the equations are integrated over control volumes (CV) using Green Gauss divergence theorem. The gauss divergence theorem converts the volume integral of divergence of a variable into a surface integral of the variable over faces comprising the CV.

Thus, the divergence term defining the convection terms can simply be computed using the face values of variables in the CV. The face values of variables are obtained from their neighboring cell centered values by using convective scheme. In this work, all the equations (except k and turbulence equations) use second order linear discretization scheme, while the turbulent equations use linear upwind convection schemes. Similarly, the diffusion term involving Laplacian operator (the divergence of the gradient) is simplified to computing the gradient of the variable at the face. The gradient term can be split into contribution from the orthogonal part and the non-orthogonal parts, and both these contributions are accounted for. The mesh details, CFD domain set up, boundary and initial conditions for the three different approaches (2D,2.5D,3D) are defined below.

3.2. Simulation set up

3.2.1. Full 3D simulation:

The computational domain for a full 3D simulation is shown in Figure 1(b). The NREL blade is enclosed by a computational domain of size $160m \times 160m \times 314m$ along the flow direction X, along the span-wise direction Y and along the blade length direction Z respectively. The domain size ensures that the boundaries are located at a distance of about 30 times the maximum chord-length from the blade so as to limit influence of induced velocities and far-field boundary influences on the flow characteristics close to the blade. A uniform wind profile of $20m/s$ is applied as the inlet condition. A grid sensitivity study (between three different hexahedral dominated grids in Figure 2) reveals that as one moves towards the finest grid of 13 million cells (on right of Figure 2)), the errors in predicted forces reduce (results not shown here) for DU35 and DU40 segments but has no major influence at NACA64 and DU21 segments (as here all 3 grids gave similar results). The reasons could be attributed to flow-complexities in these segments as discussed in the section 4. For the finest mesh, there is still some divergence from reported measured forces as seen in results section (section 4). For more accurate force prediction closer to measured ones, a Large Eddy Simulation turbulence model with much finer grid will be needed (which will be computationally intensive for an industrial scale turbine). However, the current highly refined grid with $k-\omega$ SST turbulence model should be adequate for meeting the objectives of the current work. The planes used in Figure 2 are perpendicular to the blade and parallel to the stream-wise direction. The grid is finer near the blade geometry and in regions where wakes and high shear regions are expected (behind the blades). The finest grid size is $0.0125m$ near the blades and largest grid size is $0.4m$ in regions far away from the blade. The turbine-blades has a no-slip wall boundary condition. The average y^+ value near blade wall is 221, with minimum value being 0.8 and max value being 1122. For this wide range, a wall function based on Spalding's law [13] that gives a continuous kinematic viscosity profile to the wall is used. The simulations are carried out till the time the drag and lift coefficients either converged to a value or they settled to fluctuate around a mean value. For regions away from the hub and at lower angle of attack (like NACA64 and DU21), the drag and lift values converged to a constant value but for regions near the hub, they fluctuated around a mean value.

3.2.2. 2D simulation:

The flow is simulated only along the 2D planes shown in Figure 1(b). The mesh-resolution is similar to the finest mesh in Figure 2. A total of 4 simulations, one for each plane is done. The mesh-size is similar to 3D case and so are the boundary conditions at wall and inlet.

3.2.3. 2.5D simulation:

The flow is simulated independently at four 3D segments instead of a full-scale 3D blade. The segments are clipped from the full-scale 3D geometry. The mesh-resolution is similar to 3D case and so are the boundary conditions at wall and inlet. The side wall parallel to incoming flow have slip boundary conditions.

4. Results and discussions

Figures 4-7 compares flow-patterns at four sections of the flow-pattern (as predicted by 3D, 2.5D and 2D approach). The drag and lift coefficients predictions from the 2D simulation results have been compared with measured profiles from DOWEC report[2] (as shown in Figure 8). The validation in figure 8 shows that in regions away from hub (at NACA64), the 2D simulated lift and drag coefficient results are in close agreement with the measured results

(DOWEC report). This is because the flow is mostly 2D away from hub (figure 4-7). As we move in the near hub region at DU40, the 2D results deviates a lot from measurements as influence of 3D effect dominates. Figure 4-7 shows the increase in flow complexity as we move away from hub. The measured force coefficients in DOWEC report can be compared only with 2D simulations owing to similarity in geometry, and the results from 3D and 2.5D cases cannot be compared to DOWEC owing to the tapering of cross-section as a result of blade design in 3D and 2.5D case. This tapering makes the flow more three dimensional and has its influence on drag and lift coefficient values (as shown in figure 9 , which shows comparison of predictions by 3D Vs 2.5D Vs 2D). The discussions on predicted drag-lift coefficients and predicted flow pattern by the 3 approaches at the four segments are as follows :

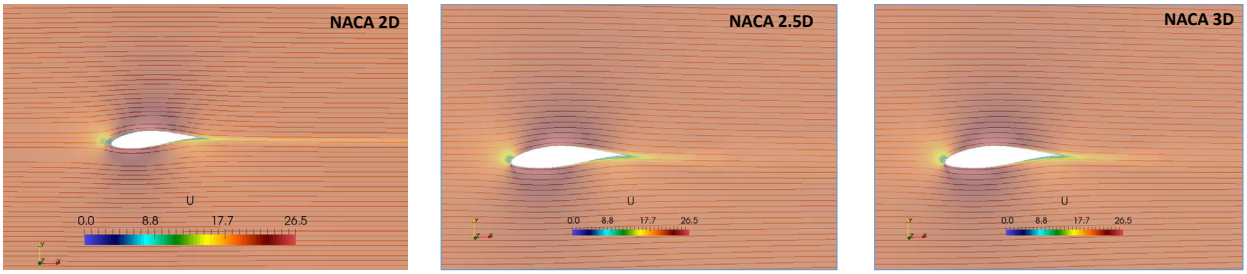

Fig. 4. Comparison of flow-pattern (velocity contour with superimposed streamlines) for 3D Vs 2.5D Vs 2D simulation at NACA64 section located 44.5m from the hub.

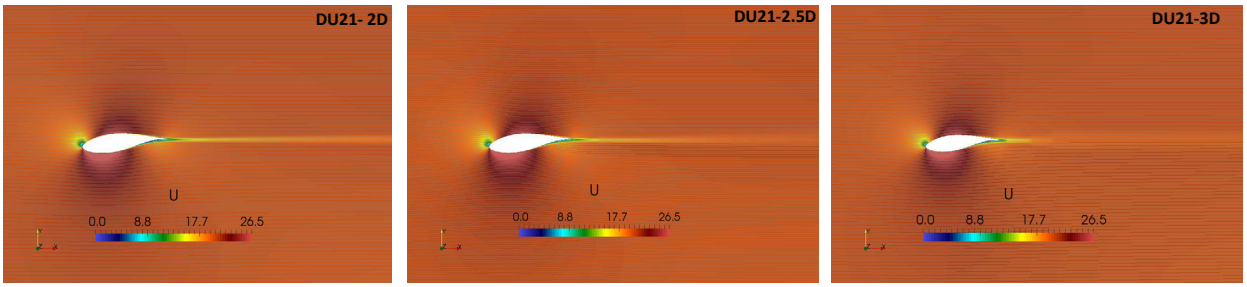

Fig. 5. Comparison of flow-pattern (velocity contour with superimposed streamlines) for 3D Vs 2.5D Vs 2D simulation at DU21 section located 36.5m from the hub.

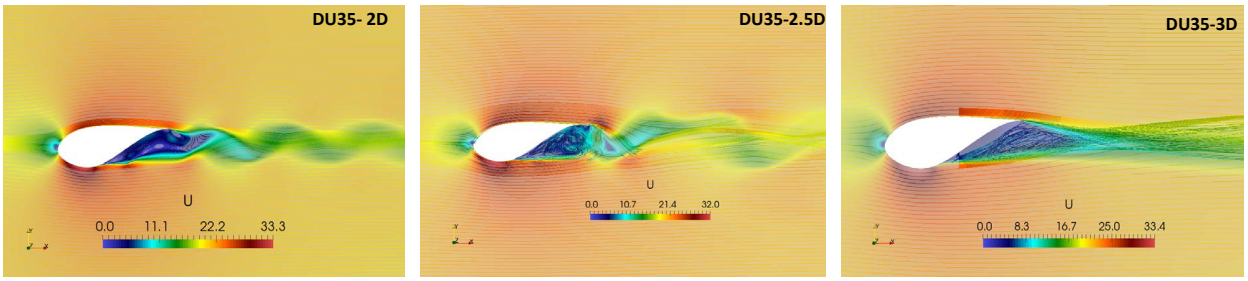

Fig. 6. Comparison of flow-pattern (velocity contour with superimposed streamlines) for 3D Vs 2.5D Vs 2D simulation at DU35 section located 15.5m from the hub.

NACA airfoil profile : This airfoil profile is located farthest from the hub (at $z = 44.5m$) with an angle of attack of $3.12°$ (figure 3) and it experience a streamlined flow as seen in Figure 4. The plot compares flow-patterns (velocity contour with superimposed streamlines) for 3D, 2.5D, 2D simulations at the NACA64 section of the blade. It is evident from Figure 4 that there is negligible difference between the three simulations (2D, 2.5D, 3D), implying, a lack of three dimensionality and associated unsteadiness in the flow behavior. This can be attributed to the aerodynamic shape of the NACA64 profile and the low angle of attack in combination to its location far away from the hub where the

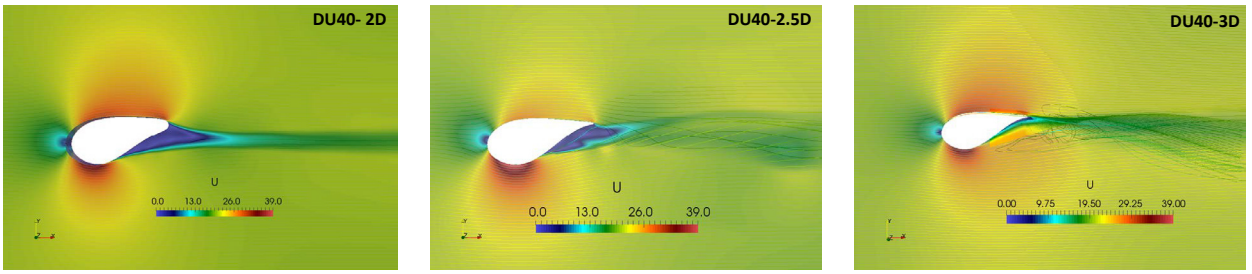

Fig. 7. Comparison of flow-pattern (velocity contour with streamlines) for 3D Vs 2.5D Vs 2D simulation at DU40 section located 11.75m from the hub.

geometry is more bluff. All the simulations converge to almost a single value of drag (C_d = 0.01) and lift (C_l = 0.1) coefficient as shown in the figures 9. Absence of oscillation in the computed values of these coefficients also confirms the absence of flow separation and associated vortex shedding.

DU21 airfoil segment : This profile is located at a distance of 36.5m from the hub center at an angle of attack of 5.3° (figure 3). Similar to the behavior shown by NACA64 section, the flow is streamlined and strongly attached to the blade section, as shown in the Figure 5. No significant differences are observed between the three simulations and the predicted values of drag and lift coefficients are 0.01 and 0.2 respectively (figures 9(a) and 9(b)). The slightly higher value of the lift coefficient compared to that experienced by the NACA64 section can be mostly attributed to the slightly higher angle of attack. The outer section of blade is designed to produce maximum torque, therefore, less separation is desirable. With the NACA64 and DU21 sections located furthest away under higher relative wind speeds increase the aerodynamic efficiency. Also both sections offer large stall point and are less likely to undergo dramatic reduction in lift to degrade the performance of the wind turbine.

DU35 airfoil segment :Figure 6 compares velocity contours with streamlines for 2D, 2.5D, 3D simulations at DU35 section located 15.5m from the hub. The streamlines (figure 6) in the 3D simulation reveal a more complex 3D flow pattern beneath the airfoil surface. 2D and 2.5D results also show a flow-separation, where as 2D show lesser chaotic streamlines than the 2.5D and 3D. Downstream the airfoil, snapshots of flow field have revealed a wavy velocity profile for 2.5D and 2D, where the streamlines emerging from the top and bottom surface of the airfoil does not cross each other and mingle. On the other hand in the 3D simulations, the wavy profile is not observed but streamlines emanating from the bottom and top of the airfoil cross-each other behind the airfoil implying three dimensionality in the flow. This intermingling of the streamlines in 3D flow combined with expected higher turbulence possibly diffuses the velocity profile. The flow-separation and three dimensional nature of the flow causes huge variations in the predicted drag force. 2D and 2.5D predict a drag coefficient of nearly 0.11 whereas the 3D predicts a drag of around 0.09 (see figure 9(a)). The simulated drag coefficient for DU35 is higher than NACA64 and DU21. In comparison to the NACA64 and DU21 sections, the 2D and 2.5D simulations for the DU35 section predict higher drag coefficients (Figure 9(a)). Comparison of the lift coefficient (Figure 9(b)), again has shown a wide variation in the predicted values with all the three approaches. Furthermore, the 2D simulation altogether failed to predict the trend ie. increase in negative lift coefficient while moving from turbine tip towards the hub.

DU40 airfoil segment : The DU40 airfoil is the closest section to the hub that has been studied (at z = 11.75m) with highest angle of attack of 13.3°. Here, the reported drag and lift coefficient values are higher in magnitude than the simulated values for DU35, DU21 and NACA64. Similar to DU35, the DU40 case also have shown a high variations in the predicted drag and lift coefficient values from the three approaches (as seen in figure 9(a) and figure 9(b)). Here, 2D predicts highest drag coefficient and lowest lift coefficient for DU40 (amongst 3D and 2.5D). This could be because 2D predicts a larger wake (suggesting higher form-drag acting in stream-wise direction) as compared to 2.5D and 3D case (see figure 7) but the low-lift could be because of two factors : a balanced pressure distribution profile around airfoil and due to the fact that the streamlines emerging from airfoil's bottom do not bend upwards as in case of 3D and 2.5D (indicating a low reactive downward lift on the airfoil for 2D case). The difference in the wake and streamlines behavior between 2D and 2.5D-3D is shown in figure 7.

This work has been able to identify the impact of bluffness of turbine-geometry and comparative predictive ability of a 2D Vs 2.5D vs 3D simulation. The results indicate that even for a non-rotating blade (in stand-still aerodynamic

condition), the blade-segments nearer to the hub, the flow is dominated by complex 3D structures and as one moves away towards blade segments located towards the tip, the flow begins to loose its 3D characteristics and can be reasonably well represented by efficient 2D simulations. Since the outer part of the blade makes a significant contribution to the total torque generated, a 2D approach might be sufficient to predict torque and associated power reasonably well. However, a 3D approach will still be required to predict structural failure and design more efficient and robust blades.

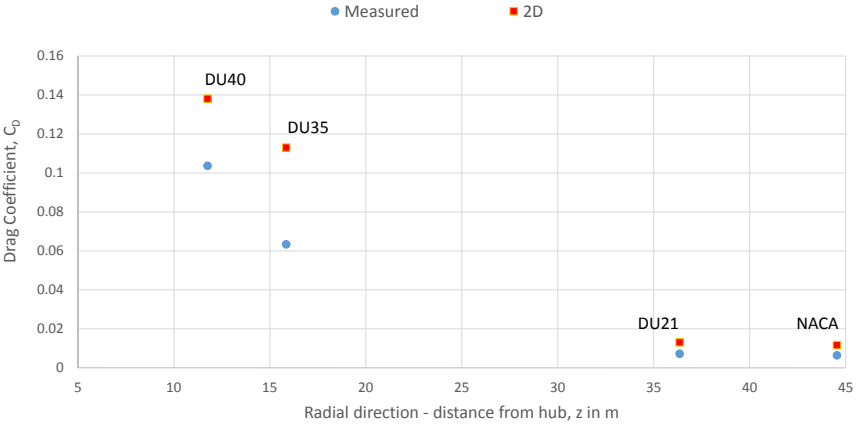

(a) Drag Coefficient

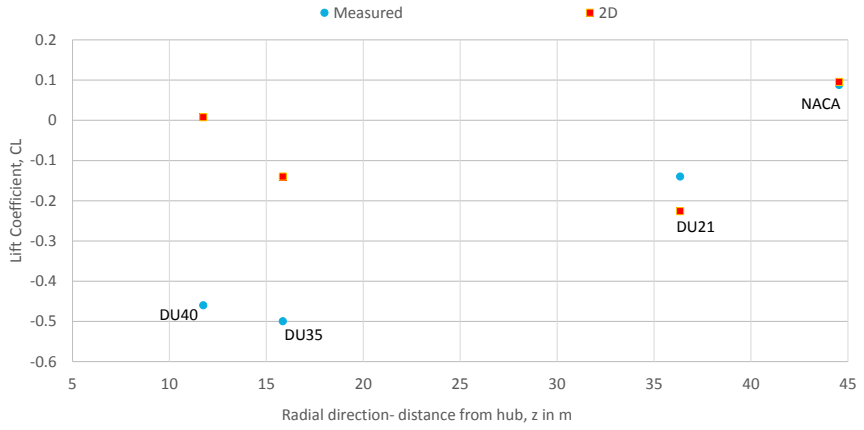

(b) Lift coefficient

Fig. 8. Comparison of drag and lift coefficient prediction from 2D with DOWEC Report.

5. Conclusion

Flow characteristics around a full scale blade of an NREL 5MW turbine is investigated using full fledged 3D, 2.5D and 2D simulations. The most important conclusions can be highlighted as follows:

- The flow close to the hub is dominated by complex 3D structures while as one recedes away from the hub, the flow starts to loose its 3D characteristics and can be reasonably well represented by efficient 2D simulations.
- For NACA64 and DU-21 sections, the three approaches predict similar values of drag and lift coefficients, which is attributed to the two dimensionality of flow in these regions away from the hub. The 2D results are also in good agreement with the experimentally measured values reported in DOWEC.

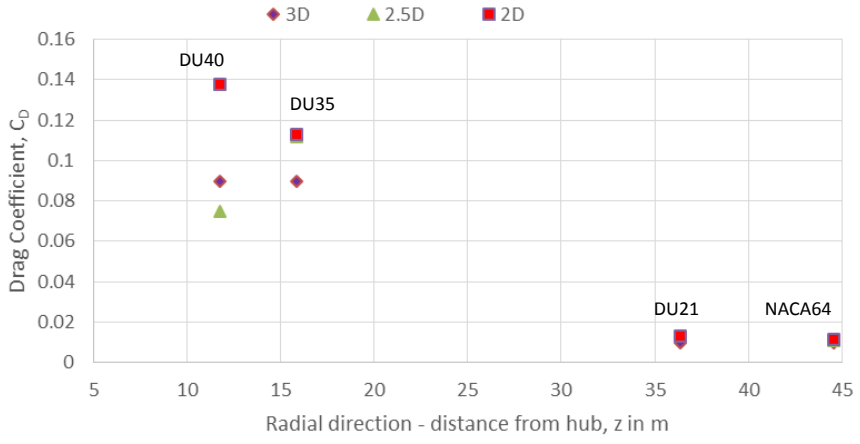

(a) Drag Coefficient

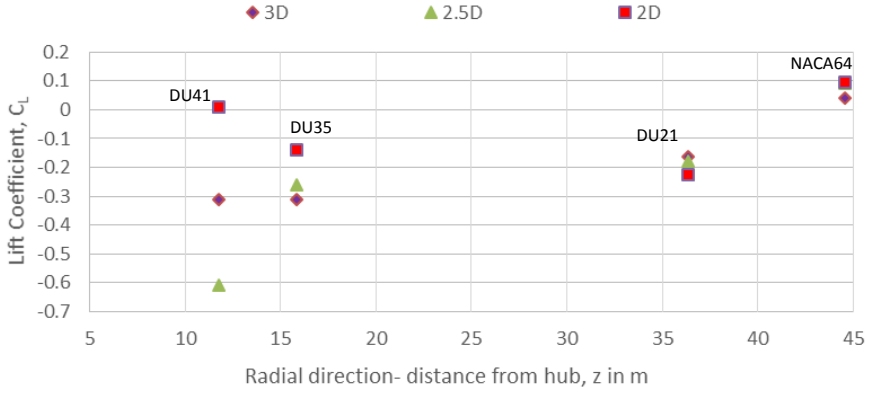

(b) Lift coefficient

Fig. 9. Comparison of drag and lift coefficient prediction from 3D,2.5D and 2D

- For DU-35 and DU-40 sections, the three approaches predict different values of drag and lift coefficients, which is attributed to the three dimensionality of flow in these regions near to the hub. The 2D simulation results also deviate from the experimentally measured values from DOWEC report.

In spite of the limitations of the 2D simulation results at near hub regions, there is a silver lining. It is well established that the major torque contribution comes from the outer part of the blade, where the flow exhibits two dimensional behavior. So for the purpose of estimating power production at a wind farm scale, the applicability of simplified approaches based on strip-theory and BEM with tip-loss corrections can still be defended. However, their applicability for structural load predictions and blade design optimization might still be questionable. Another point worth highlighting is that the current study is conducted for a stationary blade, while the blades are optimized for rotating conditions. A similar investigation for a full scale rotating turbine needs to be conducted in future as the rotating turbines adds to flow complexity in its own way.

Acknowledgements

The authors would like to acknowledge the financial support from the Norwegian Research Council and the industrial partners of the FSI-WT (http://www.fsi-wt.no) project (Kjeller Vindteknikk, Statoil, Trønder Energi AS and WindSim).

References

[1] Opstal TV, Fonn E, Holdahl R., Kvamsdal T, Kvarving AM, Mathisen KM, Nordanger K, Okstad KM, Rasheed A, Tabib M. Isogeometric methods for CFD and FSI-simulation of flow around turbine blades. Energy Procedia, Volume 80, 2015, 442449.

[2] Kooijman, H. J. T., Lindenburg, C., Winkelaar, D., and van der Hooft, E. L. 2003. DOWEC 6 MW Pre-Design: Aero-elastic modeling of the DOWEC 6 MW pre-design in PHATAS, DOWEC Dutch Offshore Wind Energy Converter 19972003 Public Reports , DOWEC 10046-009, ECN-CX–01-135, Petten, the Netherlands: Energy Research Center of the Netherlands.

[3] M. Bastankhah and F. Port-Agel. 2015. A wind-tunnel investigation of wind-turbine wakes in yawed conditions, in Journal of Physics: Conference Series, vol. 625.

[4] Siddiqui, M., Rasheed, A., Kvamsdal. T., Tabib M. V. 2015. Three Dimensional Variable Turbulent Intensity Flow Field Characterization of a Vertical Axis Wind Turbine. Energy Procedia, Volume 80, 312320.

[5] Churchfield MJ, Lee S, Moriarty PJ, Martnez LA, Leonardi S, Vijayakumar G, Brasseur JG, A large-eddy simulation of wind-plant aerodynamics, 50th AIAA Aerospace Sciences Meeting Including the New Horizons Forum and Aerospace Exposition, 2012

[6] Tabib M, Rasheed A, and Kvamsdal T. Investigation of the impact of wakes and stratification on the performance of an onshore wind farm. Energy Procedia, Volume 80, 2015, 302311.

[7] Kvamsdal T, Fonn E, Kvarving AM, Mathisen KM, Nordanger K, Okstad KM, Opstal Tv, Rasheed, A and Tabib, M. V. 2015. Strip theory approach for FSI of offshore wind turbine blades, VI International Conference on Coupled Problems in Science and Engineering, Venice, 2015.

[8] Madsen, H., Mikkelsen, A., ye, S., Bak, C., and J Johansen. 2007 . A detailed investigation of the Blade Element Momentum (BEM) model based on analytical and numerical results and proposal for modifications of the BEM model. J. Physics: Conference series 75.

[9] Dssing M., Madsen, H. and Bak, C. 2012. Aerodynamic optimization of wind turbine rotors using a blade element momentum method with corrections for wake rotation and expansion. Wind Energy 15(4)

[10] Jonkman, H., Butterfield, J., Musial, W., Scott, G. 2009 . Definition of a 5-MW reference wind turbine for offshore system development. Technical Report NREL/TP-500-38060, National Renewable Energy Laboratory, Golden, CO, 2009.

[11] Menter, F. R., Esch, T. 2001. Elements of Industrial Heat Transfer Prediction. 16th Brazilian Congress of Mechanical Engineering (COBEM).

[12] Hellsten, A. 1998. Some Improvements in Menter's k-omega-SST turbulence model. 29th AIAA Fluid Dynamics Conference, AIAA-98-2554.

[13] Spalding D. 1961.A single formula for the law of the wall. *Transactions ofth ASIDE, Series E: Journal of Applied Mechanics* 28,455-458.